Journal of Power Sources 206 (2012) 245–252

Contents lists available at SciVerse ScienceDirect

Journal of Power Sources

journal homepage: www.elsevier.com/locate/jpowsour

Investigation on the part played by the solid electrolyte interphase on the electrochemical performances of the silicon electrode for lithium-ion batteries

M. Ulldemolins[a,b], F. Le Cras[a,*], B. Pecquenard[b], V.P. Phan[b,c], L. Martin[a,d], H. Martinez[d]

[a] CEA LITEN, 17 Rue des Martyrs, F-38054 Grenoble, France
[b] CNRS, Université de Bordeaux, ICMCB Site de l'ENSCBP, 87 Avenue du Dr. Schweitzer, 33608 Pessac cedex, France
[c] STMicroelectronics, Advanced Technologies R&D, IMS/ASD & IPAD Division, 16 rue Pierre et Marie Curie, B.P. 7155, 37071 Tours Cedex 2, France
[d] IPREM ECP–UMR CNRS 5254, Université de Pau et des Pays de l'Adour, Hélioparc Pau-Pyrénées, 2 Avenue du Président Angot, 64053 Pau Cedex 9, France

ARTICLE INFO

Article history:
Received 23 November 2011
Received in revised form 10 January 2012
Accepted 13 January 2012
Available online 23 January 2012

Keywords:
Silicon
Lithium-ion battery
Thin film
Vinylene carbonate
Electrolyte additive
SEI layer

ABSTRACT

Silicon which has a theoretical capacity around 3500 mAh g^{-1} and low insertion/deinsertion potentials is one of the most promising candidates to replace graphite as a negative electrode in lithium-ion batteries. Electrochemical performances of Si electrodes are highly dependent on the quality of the SEI. Therefore, the effect of an electrolyte additive, the vinylene carbonate (VC) on electrochemical performances was investigated on sputtered silicon thin films which constitute a simple system (avoiding the use of binders or any conducting additive material). The addition of only 2% of VC significantly improves the capacity retention as well as the coulombic efficiency leading to a capacity retention of 84% after 500 cycles and a coulombic efficiency around 99.5%. To explain the behaviour differences, thorough electrochemical analyses (capacity, coulombic efficiency, polarization at half charge...) combined with scanning electron and atomic force microscopies were carried out. Some correlations have been established between the electrochemical performances and the morphology evolution of the electrode. Thus, VC limits the formation of cracks induced by repeated expansion/contraction cycles and the liquid electrolyte/electrode interactions. In addition, the mechanical pressure locally applied to the thin film allows to maintain a dense morphology and hence has a beneficial effect, too. These two key parameters limit the deterioration of the electrode over cycles.

1. Introduction

From microelectronics to transportation and electric grid, lithium-ion batteries are widely used and have to meet drastic requirements for future applications. Because of its high theoretical specific capacity (3579 mAh g^{-1} or 834 μAh cm^{-2} $μm^{-1}$ until the $Li_{15}Si_4$ final composition) and its low working potential, silicon is a good candidate to replace graphite at the negative electrode and to enhance the energy density of Li-ion cells [1]. Nevertheless such a high capacity is accompanied by a large volume variation, at the origin of a rapid fading of electrochemical performances [2]. However, 100 nm-thick silicon thin-films have achieved excellent cycle life in all-solid state microbatteries (more than 1500 cycles without measurable capacity loss and a coulombic efficiency remaining higher than 99.99%) [3], despite this volume change. In liquid electrolyte, the electrochemical performances of the silicon electrode are strongly dependent on the electrolyte composition [4]. Because of its low working potential (<0.5 V *vs* Li/Li^+), the reduction of both the solvents and the salt of the electrolyte occurs at the electrode/electrolyte interface and generates a solid electrolyte interphase (SEI) [5,6], already intensively studied on graphite anodes [7]. Reversible cycling and long term stability is closely related to the effectiveness of the surface passivation, which depends on the SEI chemical properties and its ability to accompany the electrode morphological changes during the lithium insertion/deinsertion cycle [8]. In the case of graphite, it has been proved that these SEI properties can be enhanced by using selected additives [9–11].

A similar approach can be considered for silicon. Some additives like vinylene carbonate (VC) [12], fluoroethylene carbonate (FEC) [13], succinic anhydride (SA) [14], and more recently, tris(pentafluorophenyl) borane (TPFPB) [15] were studied with silicon-based negative electrodes. These studies mostly emphasize the beneficial effect of additives on the electrochemical performances. Indeed, a small amount of additive improves both long term cycling and coulombic efficiency. Thus, Chen et al. showed that adding 1 wt % of VC to an electrolyte containing 1 M $LiPF_6$ dissolved in a mixture of ethylene carbonate (EC) and dimethyl carbonate (DMC) in a 1:1 (v/v) ratio allows to greatly enhance the capacity retention [12]. Hence, for a 150 nm thick thin-film of silicon, around 50% of the first charge capacity remains after

* Corresponding author. Tel.: +33 438784559; fax: +33 438785117.
E-mail address: frederic.lecras@cea.fr (F. Le Cras).

0378-7753/$ – see front matter © 2012 Elsevier B.V. All rights reserved.
doi:10.1016/j.jpowsour.2012.01.095

500 cycles with almost 100% of the coulombic efficiency after 3 cycles in VC-containing electrolyte, whereas in VC-free electrolyte, charge capacity collapses under 35% of the first charge capacity after 200 cycles. Impedance spectra analysis shows that internal resistance continuously increases while cycling without VC, whereas it remains stable with VC. Similar results were obtained with FEC [13] and TPFPB [15]. SA not only improves long term cycling stability, but also tends to increase the internal resistance [14].

As the electrode/electrolyte interface is a key point to improve the electrochemical performances, this study deals with the effect of VC on the surface morphology by means of scanning electron microscopy (SEM) and atomic force microscopy (AFM). In addition to SEM analyses, AFM was used to observe the evolution of the sample morphology when using VC or not during cycling. Moreover, quantitative data could be extracted from this study as a real $(X,Y)Z$ signal is recorded from each point of the image (512×512). Then, RMS (root mean square) and SAD (surface area difference) parameters allow to observe the evolution of the surface topography. Then, electrochemical performances of silicon thin films with and without VC were thoroughly analysed in order to understand the precise effect of this additive on silicon. Some correlations have been established between morphology evolutions and the electrochemical performances. This study was achieved on sputtered silicon thin films, which constitute a simple system. This configuration allows to get more direct information on the silicon morphological evolution and electrode/electrolyte interactions, avoiding any parasitic effects or limitations which could be due to binders or conducting additive materials.

2. Experimental

2.1. Electrode preparation

Amorphous silicon thin films were prepared by radio frequency (RF) magnetron sputtering (PLASSYS MP 700). The 75.5 mm diameter target made of 99.999% pure silicon was purchased from Cerac Inc. Before deposition, a vacuum was applied into the chamber until the pressure was less than 8.10^{-5} Pa. All silicon thin films were deposited at room temperature with no intentional heating of the substrate at a nominal RF power of 75 W and a target-to-substrate distance equal to 80 cm. The films were deposited under 99.999% pure argon atmosphere with a total gas pressure of 0.5 Pa. Prior to each deposition, a pre-sputtering was systematically achieved for 15 min in order to clean the target surface. Thin films were deposited on 14 mm diameter, 17 μm thick Cu foils (99.95%). The thickness of the electrodes is either 100 nm or 500 nm (*i.e.* around 20–100 $\mu g\,cm^{-2}$)

2.2. Morphology characterization

Atomic force microscopy (AFM) imaging was performed with a MultiMode Scanning Probe Microscope (MM-SPM) from Veeco society, a controller Nanoscope IIIA and a Quadrex. This microscope was placed in a glove box (argon atmosphere) in order to avoid any surface contamination of the samples during analyses (oxygen and water levels being lower than 1 ppm). A preliminary study was done by optimizing the working conditions to get an optimal definition of every image details. All AFM images were acquired in intermittent contact mode (tapping) to obtain topographic (with a scanning frequency from 0.4 to 1 Hz), phase and deflection (error signal) images using a MPP-11100 Veeco probe which has a quoted probe radius of curvature lower than 10 nm. A phosphorus (n) doped Si with a force of $5\,N\,m^{-1}$ at a resonance frequency of about 150 kHz was employed. The surface roughness was determined with the use of the so-called RMS roughness R_q which can be defined as the standard deviation of the Z (height) within a given area. Additional information concerning the surface morphology is given by the SAD defined as:

$$SAD\,(\%) = \frac{\text{surface area} - \text{projected area}}{\text{projected area}} \times 100$$

Each parameter is calculated from several zones of the sample by taking into account ten measurements with a typical deviation of 5%.

SEM images of surfaces were obtained with on a JEOL 6700-F FEG-SEM on Si thin films deposited on copper substrates, previously covered by a gold thin film to avoid any charging effect.

Thin film cross-section observations were conducted of a FIB FEI Starta 400S. 2 kV and 10 pA conditions were used for the final ionic polishing step. The cross-section plane tilt *vs* the electron beam axis was 38°, consequently vertical and horizontal scales are different on SEM pictures.

2.3. Electrochemical measurements

Electrochemical characterizations were performed in CR2032-type coin cells containing the working electrode. The counter electrode was a lithium foil (Chemetall, battery grade), the electrolyte was 1 M $LiPF_6$ in a 1:1:3 volumetric mixture of ethylene carbonate (EC), propylene carbonate (PC) and dimethyl carbonate (DMC), with and without 2 wt% of vinylene carbonate (VC) (Novolyte). A polypropylene microporous membrane (Celgard 2400) associated with a non-woven polypropylene felt (Viledon, Freudenberg) was used as separator. The electrochemical experiments were carried out on a VMP galvanostat/potentiostat (Bio-Logic). Discharges and charges were performed in galvanostatic mode between 0 V and 1 V *vs* Li^+/Li under a constant current density of $100\,\mu A{\cdot}cm^{-2}$. All Si electrodes were dismantled and washed with fresh DMC to remove residual electrolyte solvents and salt. Cell assembly, disassembly and electrode washing processes were carried out in an argon filled glove box. Samples were packaged in airtight glass tubes under argon and introduced in the glove box of the corresponding characterization apparatus (AFM) or transferred through an airtight system into the scanning electron microscope chamber. All analyses were carried out onto the pristine Si thin film and at different stages of the cycling.

3. Results

3.1. Electrochemical performances

As shown in Fig. 1a, silicon thin film electrodes exhibit improved cycle life and higher coulombic efficiency when cycled in a VC-containing electrolyte. The thickness of the film does not modify this tendency (Fig. 1b), but thinner films deliver higher initial capacities due to a decrease of the lithium diffusion length, and their capacity fading is clearly delayed with VC. In the case of 500 nm thick films, 84% of the capacity retention is obtained after 500 cycles in VC-containing electrolyte and the coulombic efficiency is higher than 99% after the second cycle (Fig. 1a). In contrast, in VC-free electrolyte, after reaching a maximum after a few tens of cycles (depending on the thickness of the electrode), the capacity dramatically collapses reaching 50% of its maximum value after 70 cycles, and less than 20% after 150 cycles, this evolution is associated with a fluctuating and quite low coulombic efficiency. Whereas initial coulombic efficiencies are almost the same with and without VC for the three first cycles, some major differences are observed for the following cycles. Initial capacities are lower than the theoretical one because of operating conditions. Indeed, even if discharges were carried out down to 0 V *vs* Li^+/Li, current rate is

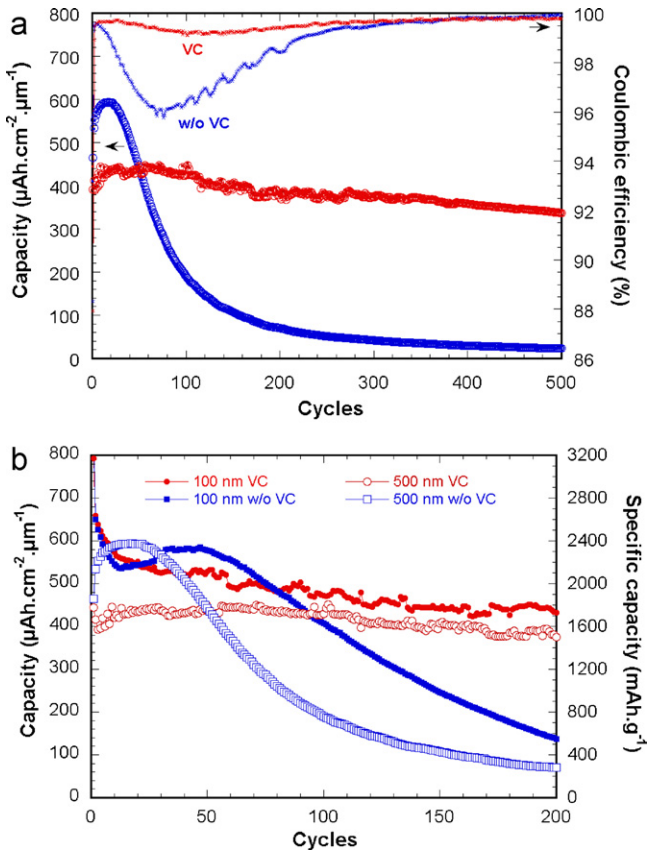

Fig. 1. (a) Comparison of capacity retention and coulombic efficiency of 500 nm-thick Si thin film electrodes (red) with VC and (blue) without VC. Hollow and solid marks represent discharged and charged capacities, respectively. b) Comparison of cycle performance of 100 nm and 500 nm-thick Si thin film electrodes (red) with VC and (blue) without VC. (For interpretation of the references to colour in this figure legend, the reader is referred to the web version of the article.)

higher than C/3 (based on experimental capacities), and no voltage floating is applied. Moreover, it is well known that the lithium diffusion coefficient in silicon is very low [3], leading to a lithium concentration gradient inside the electrode. Hence, the part of the active material which is close to the electrode/electrolyte interface is rapidly saturated with lithium whereas the core of the silicon electrode remains less lithiated. Thus, the working electrode is reaching the cut-off voltage without being fully lithiated.

The voltage curves corresponding to the first six cycles are represented in Fig. 2. During the first cycle, there is no clear difference brought by VC additive. The shape of the voltage curve exhibiting a low insertion step under 150 mV, the amounts of inserted then deinserted lithium, and consequently the irreversible capacity, are almost the same with both electrolytes. A difference in behaviour starts appearing between the two electrolytes during the second lithium insertion and becomes more obvious during subsequent cycles. For one, the amount of inserted lithium at each cycle rapidly increases without VC (+15% between the first and the second discharge), whereas it remains quite stable or slightly decreases with VC. For another, the previous behaviour is connected to an evolution of the discharge curve shape. Indeed, while the voltage profile coincides at the beginning of the discharge for both electrolytes, a sudden drop of the voltage occurs in the second part of the discharge with VC, whereas the decrease in the voltage until the cut-off is more progressive without VC. Moreover, one can notice that the last part of the discharge curve observed for further cycles with VC gets back to the initial discharge curve located at a

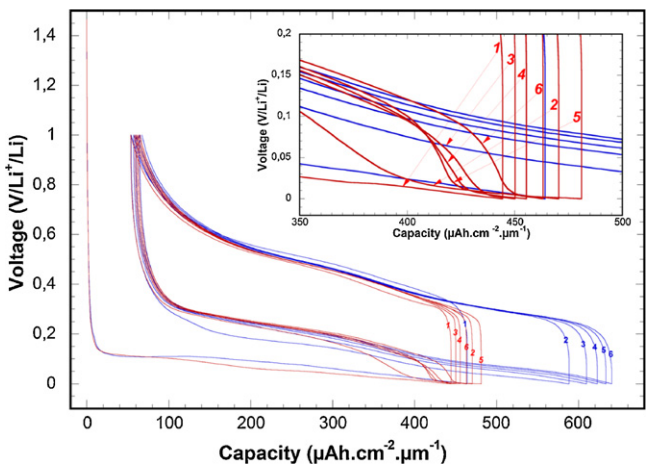

Fig. 2. First galvanostatic cycles (from 1 to 6) of 500 nm thick Si thin film electrodes with VC (red) and without VC (blue). The current density is 100 µA cm^{-2}. (For interpretation of the references to colour in this figure legend, the reader is referred to the web version of the article.)

lower voltage. Finally, contrary to the discharge, the voltage profile of the charge with VC fully superimposes with the one without VC.

The presence of this surprising voltage step between about 100 mV and 20 mV during the lithium insertion in the electrolyte containing VC is not likely to be attributed to a new electrochemical reaction specific to the presence of VC. Indeed, the coulombic efficiency which is measured (~99.5%) is too high and the SEI formation is known to occur above 1.0 V *vs* Li^+/Li in the presence of VC [9].

Upon further cycles, the shape of the voltage curve either in charge or in discharge remains unchanged in the presence of VC (Fig. 3), the steep voltage drop being still present at the end of the lithium insertion. On the contrary without VC (Fig. 4), the voltage curve evolves as the capacity rapidly fades.

3.2. Morphology evolution

SEM images of the copper substrate and a dense pristine silicon thin film (Fig. 5) show that the deposition is conformal with the pyramid-patterned surface of the copper foil. AFM measurements performed on both samples are consistent with these observations, indicating that R_q and SAD (around 28%) are similar. A slightly lower roughness for the Si electrode (723 nm instead of 816 nm for the

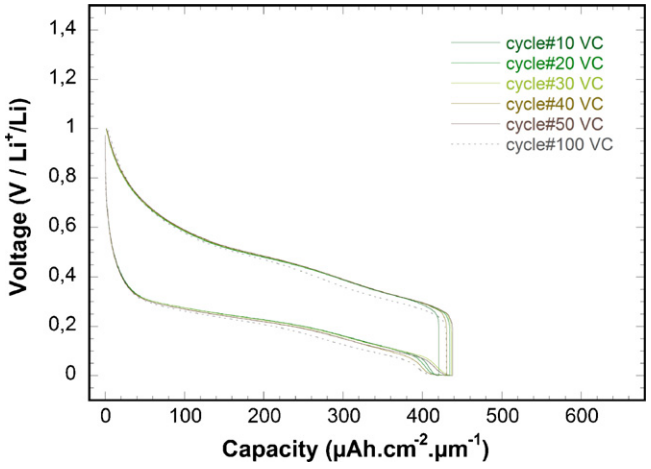

Fig. 3. Evolution of the voltage curve of a 500 nm thick Si thin film electrode cycled with VC from the 10th to the 100th cycle. Some cycles were selected to facilitate the understanding.

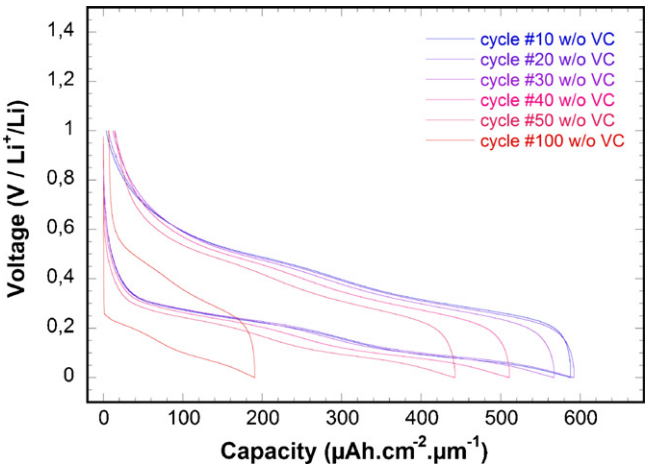

Fig. 4. Evolution of the voltage curve of a 500 nm thick Si thin film electrode cycled without VC from the 10th to the 100th cycle.

substrate alone) indicates that the deposit has partially filled valleys between hills.

At the end of the first lithium insertion (discharge), as expected, the silicon film has swollen in both cases (Fig. 6a and e). At this stage, there is no influence of the additive on the global morphology of the electrode. Then, at the end of the first charge, damages accompanying the layer shrinkage are clearly visible: large cracks are formed in the film without VC (Fig. 6f) whereas they seem to be less present with VC (Fig. 6b). The formation of a surface film is clearly visible on the top of the electrode cycled with VC which probably hides or at least levels similar subjacent cracks as those observed without VC.

Subsequent cycles lead to the formation of Si islets alternatively swelling and shrinking, but remaining anchored at the surface of the current collector. At the end of the 30th discharge (Fig. 6c and g), thin films are still swollen with more cracks and a higher roughness than after the first discharge. We can also notice that residual voids resulting from cracks are more visible when cycled in VC-free electrolyte. At the end of the 30th charge (Fig. 6d and h), well-defined contracted Li_xSi islets, surrounded by large voids revealing the surface of the Cu substrate, are present. But, no obvious differences are visible at this stage after 30 complete cycles between the two types of electrolytes on the SEM images. Nevertheless, a morphology difference between the two types of cycled electrode can be quantified by AFM measurements which show a far larger increase of both the electrode roughness and the actual surface area without VC (Fig. 7). Hence, the SAD varies from 61.2% with VC to 81.6% without VC, and the electrode roughness from 886 nm with VC to 1132 nm without VC. From a SEM image of the thin film cross-section obtained at the end of the 30th charge, the thickness of the electrode was estimated to a value higher than 2 µm while the pristine electrode is only 500 nm thick.

At the end of the 500th charge (Fig. 8), the surface of electrodes is dramatically modified by successive discharge/charge cycles, highlighting a more marked nanostructuration with a gypsum flower type morphology. Even if the differences induced by the presence of VC are not obvious, it seems that Si islets are less dispersed and then the electrode is less damaged.

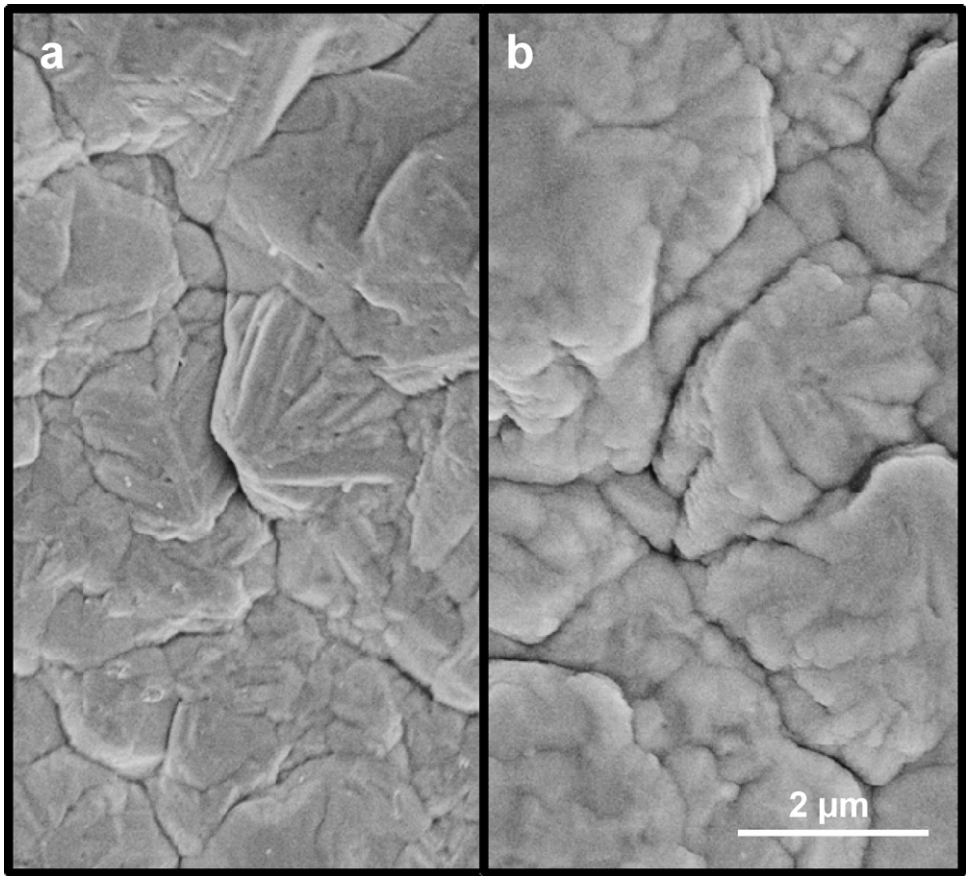

Fig. 5. SEM images of Cu substrate (a) and as-deposited 500 nm-thick Si thin film electrode (b).

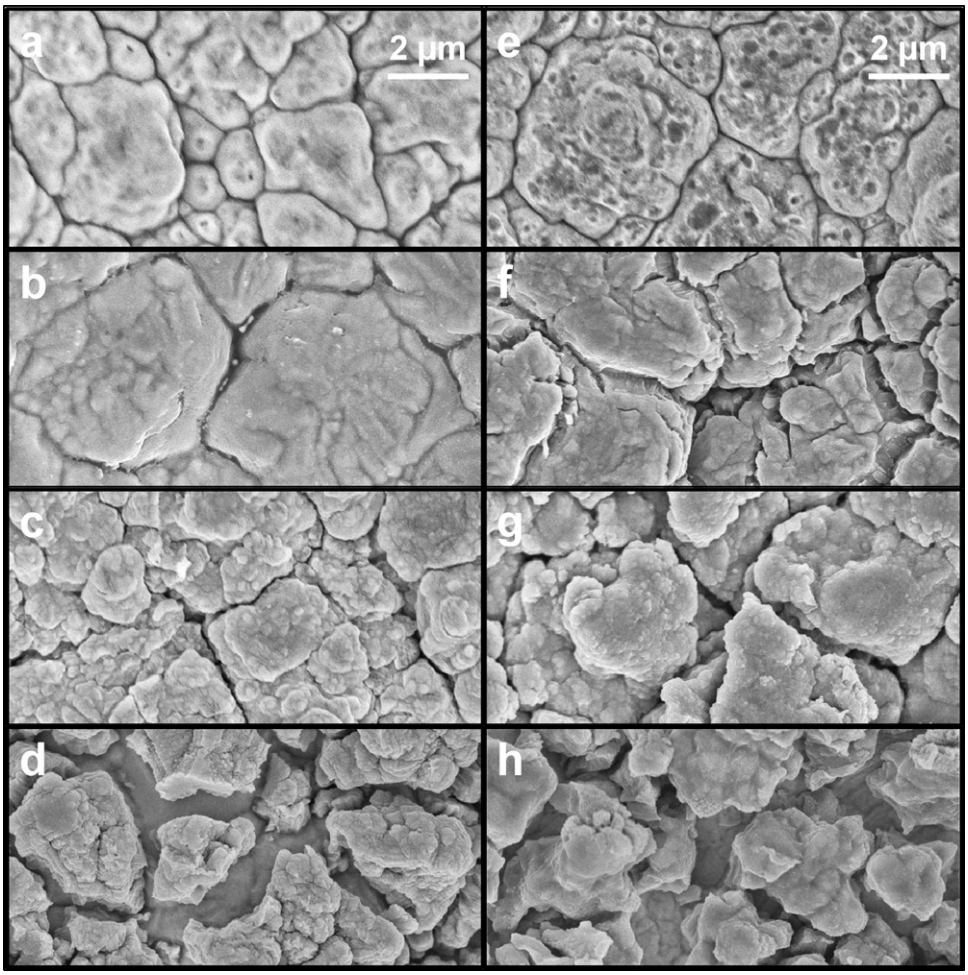

Fig. 6. SEM images of 500 nm thick Si thin film electrodes after the 1st discharge (a and e), the 1st charge (b and f), the 30th discharge (c and g), the 30th charge (d and h). On the left (from a to d), the images correspond to electrodes cycled with VC while on the right (from e to h), they are relative to electrodes cycled without VC additive.

4. Discussion

During the first cycle, there is no clear influence of the VC addition on the electrochemical behaviour of the silicon thin film. The irreversible capacity between the first lithium insertion and deinsertion, mainly attributed to the reduction of both the solvents and the lithium salt at the surface of the silicon electrode and then possibly to the formation of a SEI layer, is the same in both cases (with and without VC). It is consistent with our XPS analyses [16] which demonstrate, in agreement with the literature [17], that the addition of only 2 wt% of VC to the liquid electrolyte does not greatly modify the chemical composition of the SEI, although it has a clear filmogen effect as seen on the SEM images.

At the end of the first charge, the location of the primary cracks seems to be related to the topography of the copper current collector in both cases. Indeed, the wider cracks seem to form preferably in the 'valleys' present at the pyramid-patterned surface of the substrate: during the initial lithium insertion and swelling of the film, the Li_xSi alloy present in the bottom of the valleys is constrained and this leads to a larger local thickness of the film in this region. During the subsequent lithium extraction, the shrinkage of the film is not homogeneous at the surface which favours the initiation of cracks. Nevertheless, Li and al. showed the formation of cracks even on a flat silicon wafer substrate [18]. On their 500 nm thick film, multiple straight cracks with few sharp changes in direction were generated, forming an array of intersecting cracks. In the present case, these primary cracks formed during the lithium deinsertion step are then probably caused by both the presence of lithium concentration profile perpendicular to the substrate and the in-plane thickness inhomogeneities. Once a similar network of primary cracks is formed in both cases, the influence of VC on the electrochemical behaviour of the fractured film becomes more obvious.

When no VC is added to the electrolyte, the capacity increases rapidly during the first twenty cycles. The capacity ratios $Q_{d,cycle\ n+1}/Q_{c,cycle\ n}$ far above one and $Q_{d,cycle\ n}/Q_{c,cycle\ n}$ around unit clearly indicate that the amount of lithium able to insert in the silicon film is enhanced by the previous extraction step, whereas the amount of lithium extracted remains almost equal to the amount inserted previously (Fig. 9). Moreover, in the same time, for initial cycles (up to about 15 cycles) the difference between the voltages measured at half-capacity for the discharge and the charge at each cycle (polarization) decreases (Fig. 10). These observations are consistent with a progressive increase of the electroactive surface of the film caused by the shrinkage of the active material and the formation of new cracks during each charge (delithiation). SEM pictures confirm the progressive fracture of the matter between the first and the thirtieth cycle, and the possibility for the liquid electrolyte to deeply penetrate into the cracks. Thus, both the increase of the electrode/electrolyte contact area and the decrease of the lithium diffusion path contribute to a more efficient and complete alloying reaction. The limited amount of lithium inserted during the first discharge appears then as a consequence of the higher initial polarization, connected itself to a

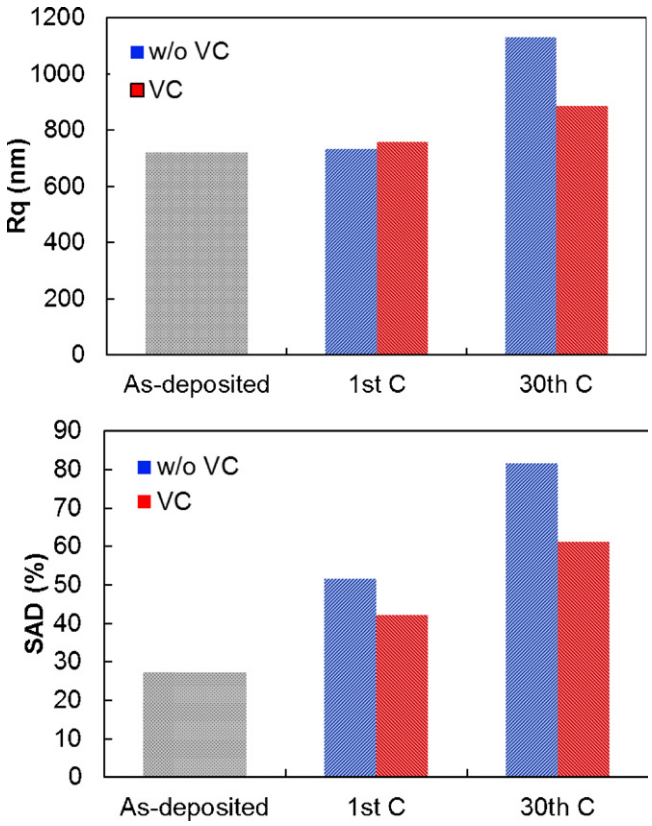

Fig. 7. Evolution of surface area difference (SAD) and roughness (R_q) of 500 nm thick Si thin film electrodes cycled with VC (red) and without VC (blue). (For interpretation of the references to colour in this figure legend, the reader is referred to the web version of the article.)

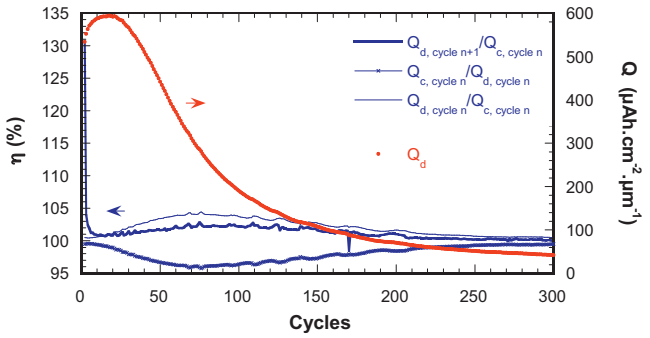

Fig. 9. Evolution of the discharge/charge capacity ratio ($Q_{d,cycle\ n}/Q_{c,cycle\ n}$; here the charge comes just after the discharge), and the discharge of the subsequent discharge/charge capacity ratio ($Q_{d,cycle\ n+1}/Q_{c,cycle\ n}$; here the discharge comes just after the charge), in VC-free electrolyte.

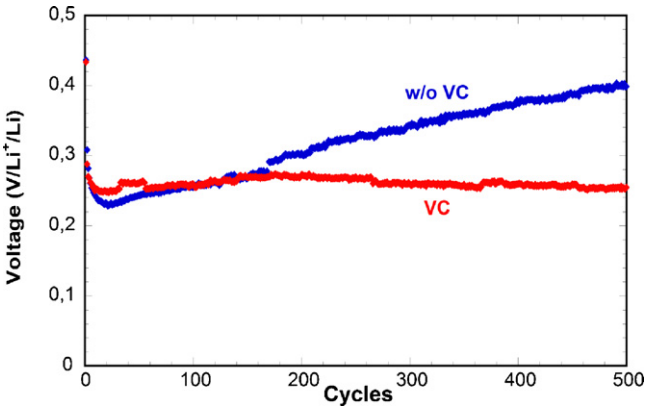

Fig. 10. Evolution of the polarization at half-capacity upon cycling, with (red) and without VC (blue). (For interpretation of the references to colour in this figure legend, the reader is referred to the web version of the article.)

higher actual current density and a longer diffusion path (thickness of the film). SEI products with identical composition continue to precipitate on fresh Si surfaces, the presence of some solid and incompressible matter inside the cracks possibly favouring their propagation and the overall morphological change of the active material.

On subsequent cycles (>20), the capacity rapidly fades. Nevertheless, the representation using a normalized capacity (Fig. 11) shows that the voltage curve is actually unchanged, at least until the 50th cycle. Both the main insertion steps around 300 mV and 80 mV *vs* Li^+/Li are present, their relative capacities remaining the same. Consequently, it is striking that the capacity fade in that case is essentially related to a loss of active material instead of a loss of reversibility of the insertion reaction itself. Parallel to this capacity fade, the polarization starts to increase progressively. This electrochemical behaviour and the pronounced morphological change of the active material observed by SEM between the 30th and the 500th cycle indicate that a growing part of the active material becomes progressively electrochemically inactive due to an electronic disconnection from the conductive substrate (additional measurements not presented here show that almost no extra lithium can be inserted at lower current densities or during floating

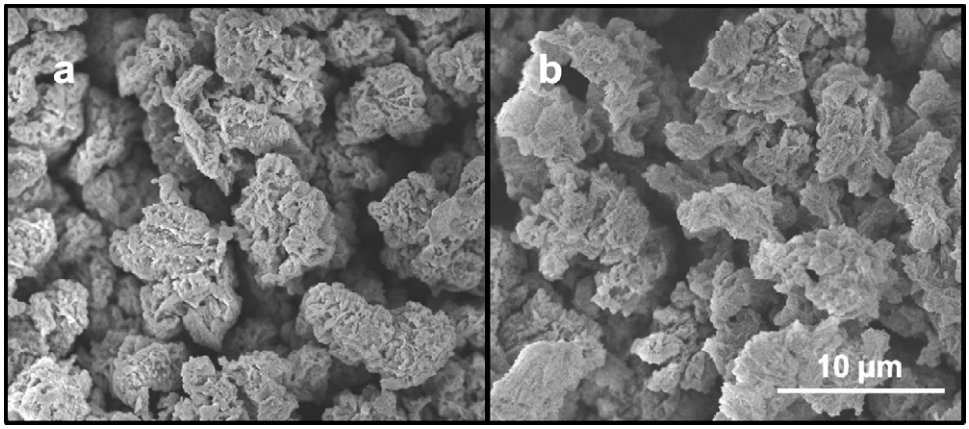

Fig. 8. SEM images of the surface of Si thin film electrodes at the end of the 500th charge cycled in VC-containing electrolyte (a) and in VC-free electrolyte (b) showing a gypsum flower type morphology.

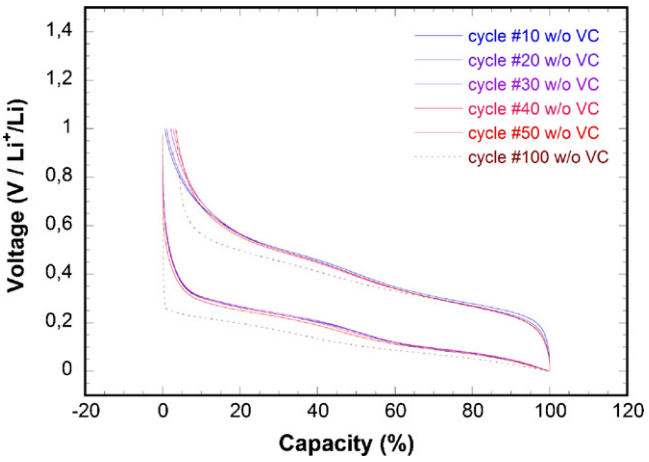

Fig. 11. Evolution of the electrochemical profile of a 500 nm thick Si thin film electrode cycled without VC from the 10th to the 100th cycle, with normalized capacity.

at 0 V *vs* Li^+/Li, thus excluding a capacity loss due to a degradation of the ionic diffusion). The amount of SEI products trapped and accumulating in the electrode (linked to the $Q_{d,cycle\ n}/Q_{c,cycle\ n}$ capacity ratio) (Fig. 9) is indeed significantly higher without VC, and would contribute to amplify the morphological evolution between each cycle as shown by AFM measurements.

Contrary to the results obtained in a VC-free electrolyte, the specific capacity early stabilizes from around the 15th cycle in the presence of the VC additive and then gently decreases to remain as high as 84% of the maximum capacity after 500 cycles. Moreover, the stabilized capacity obtained with VC is much lower than the maximum capacity obtained without VC (450 *vs* 600 $\mu Ah\,cm^{-2}\,\mu m^{-1}$), and also lower than the theoretical one (830 $\mu Ah\,cm^{-2}\,\mu m^{-1}$). But despite these differences of electrochemical behaviour, it is striking to observe no clear differences in the morphological evolution of the active material, or in the overall chemical composition of the SEI.

Nevertheless some explanations can be proposed after examining the electrochemical measurements more in depth and collating them with the morphological evolutions. As aforementioned, the limited capacity observed with VC from the second cycle is related to a sudden voltage drop occurring at the end of the insertion. This drop is followed by a stabilization at a lower voltage value, and a superimposition of the last part of the discharge curve with the discharge curve corresponding to the first insertion in the pristine dense silicon film. Besides, the SEM pictures of the film after 30 cycles in the lithiated (Fig. 6c) and delithiated states (Fig. 6d) show that, once formed, Si islets are able to swell and to shrink alternatively. In the delithiated state, large voids around the islets allow their flanks to be also in contact with the electrolyte, and consequently the lithium to diffuse from these surfaces into the material. In the lithiated state, the volume expansion fills the voids between the islets, the active surface is then reduced. The sudden voltage drop observed at the end of the discharge very likely corresponds to the closing of these lateral voids and the steep drop of the actual electrode surface. Once the voids are filled, the geometrical state of the silicon film is close to the initial one during the first insertion, the lithium only diffusing from the

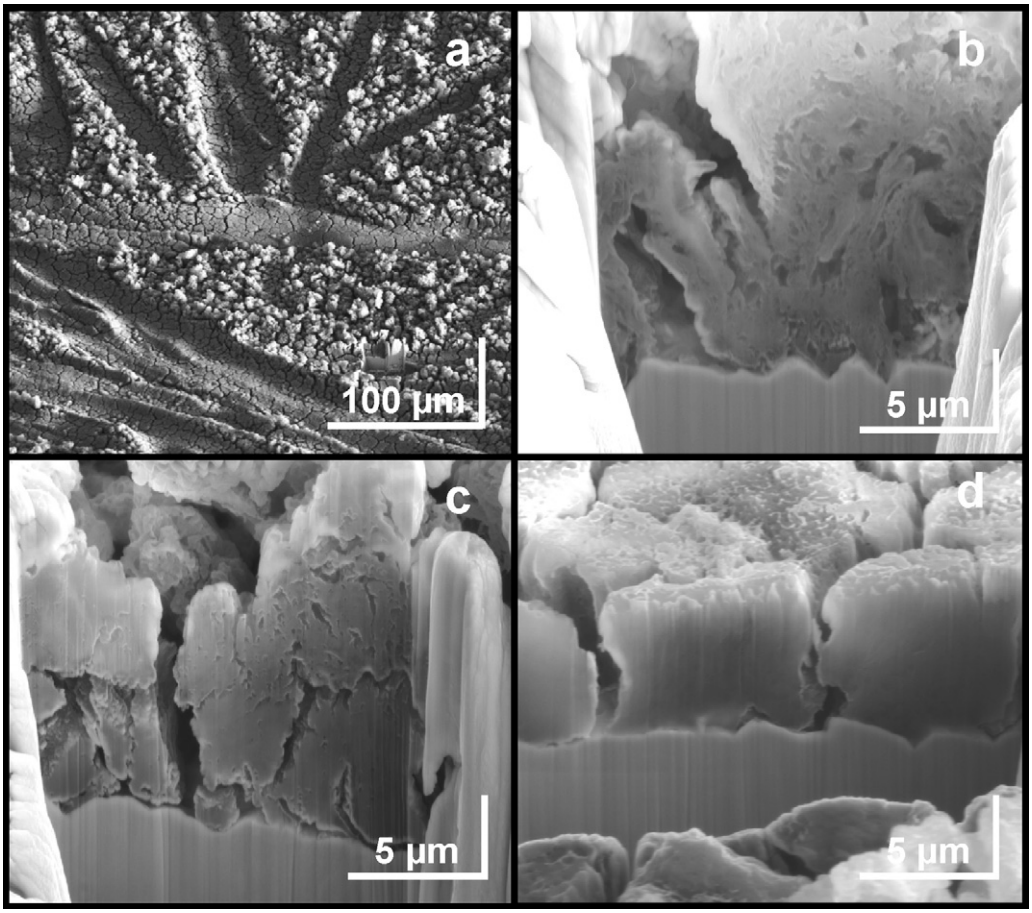

Fig. 12. SEM image of the silicon electrode surface after 500 cycles, with two distinct zones (a), and SEM images of cross-sections prepared by FIB of electrodes after 500 cycles without VC on free zone (b), with VC on free zone (c) and compressed zone (d). Horizontal and vertical scales take into account the horizontal tilt.

external surface of the film, which explains the superimposition of the end of these discharge curves.

Along the 500 cycles, the electrochemical parameters remain almost constant in presence of VC: the capacity, the polarization at half-capacity (Fig. 10), the discharge/charge capacity ratio slightly above 100%, and the shape of the voltage curve. All indicate the reversibility and the stability of the electrochemical reaction, and consequently the reversibility of the morphological changes occurring between the lithiated and delithiated state, once the primary cracks have led to the formation of silicon islets at the surface of the copper collector. Necessarily both most of the islets remain connected to the substrate and most of the silicon contained in these islets remains bound. Then, the difference of morphology observed by SEM between the 30th and the 500th cycles (Figs. 6d and 8a) with an apparent increase of the silicon fracture, should essentially deal with the surface rather than the bulk of the material.

Finally, recent SEM observations of cross-sections prepared by FIB of the electrodes after 500 cycles (Fig. 12) let clearly appear the real impact of VC on the internal microstructure of silicon islets previously deduced from the electrochemical measurements. When cycled in VC-free electrolyte (Fig. 12b), the electrode, certainly made of lithiated silicon mixed with SEI products, becomes highly porous. The "cauliflower" structuration is detrimental to both ionic and electronic conductivities, and the loose electrical contact between silicon and the copper substrate additionally contributes to the capacity fading. With VC (Fig. 12c), the internal structure of the electrode remains rather dense after 500 cycles, in spite of visible damages. In a more moderate way than without VC, the contact with the current collector is clearly reduced, but it seems sufficient to insure a quite good electronic conductivity, as proved by good electrochemical results.

Surprisingly two distinct zones were observed at the surface of the electrodes, whatever the electrolyte composition (Fig. 12a). The first zone is composed by "free" silicon surface, without any trace of exterior mechanical constraint, and the second one lets appear clear imprints of compression at the surface. These cavities are left by the PP non-woven fibres of the separator. Cross-sections image by FIB of the compressed part of the electrode cycled with VC is presented (Fig. 12d). Well-defined dense islets are visible, separated by large cracks, certainly formed during the first charge. The contact between the electrode and the current collector is clearly maintained. Even if the good capacity retention of the electrode cycled with VC is not specifically the results of these compressed areas, these observations give a clue on a way to protect the electrode from degradation. One can note that the thickness of the islets is more than ten times higher than the initial silicon thin film. The empty space between cracks is not enough to explain this difference. This might be the result of both SEI trapping and nanoporosity.

Finally, the role played by VC is the formation of a SEI which is necessarily able to prevent/to limit the contact between the liquid electrolyte and the electrode surface, even during the repeated swelling/shrinking cycles of the active material, and this implies good density and stretching ability.

In the case of composite electrodes for lithium-ion batteries, composed of silicon (nano)powder, conductive additives and binders, the improvement of the cycle life by SEI promoters will probably not be as straightforward as in this case of monolithic thin-film electrodes. Indeed, many other parameters and phenomena also influence the capacity fading of porous composite electrodes [4]: size of the Si particles and its influence on their mechanical resistance to crushing, nature of the polymer binder and its abilities to bind with the silicon surface, to accommodate the volume expansion of the electrode and to resist to fatigue stress, the choice of the carbon additives and their role as electro-active surface for the SEI formation, pore clogging due to the volume expansion of the silicon–lithium alloy and/or to the SEI growth, and so on.

Nevertheless Li_xSi/electrolyte interactions play the crucial role [19]. Consequently, the selection of electrolyte candidates through the study of the electrochemical behaviour of thin-film model electrodes should be a helpful starting point to envisage the optimization of this complex system.

5. Conclusion

Beneficial effects of VC as electrolyte additive on the operation of Si thin film model electrodes were confirmed. This system *vs* lithium is able to maintain 84% of its maximum capacity after 500 cycles, with quite high coulombic efficiency (~99.5%). A closer look at electrochemical behaviour, coupled with a morphology study, gave us precious clues to understand the part played by VC, as well as degradation mechanisms of Si electrodes. It is now clear that, after the formation of primary cracks caused by the forming of the film during the first cycles, VC limits the development of new cracks by forming an efficient SEI which limits the contact between the electrode and the liquid electrolyte. This reduces the amount of SEI products precipitating and accumulating inside the electrode at each cycle, and hence is helpful to maintain the integrity of the electrode material. The application of an external mechanical pressure at the surface of the electrode was also found to be beneficial as it contributes to maintain dense film morphology and good contact between the active material and the current collector.

Acknowledgements

The authors want to thank L. Teule-Gay and S. Gomez (ICMCB) for their help with thin film deposition and SEM characterization respectively, S. Inguanez for her precious help on VBA computing for data analysis, and A. Montani (CEA-LITEN) for conducting SEM-FIB observations.

References

[1] J.P. Maranchi, A.F. Hepp, P.M. Kumta, Electrochem. Solid-State Lett. 6 (2003) A198–A201.
[2] L.Y. Beaulieu, T.D. Hatchard, A. Bonakdarpour, M.D. Fleischauer, J.R. Dahn, J. Electrochem. Soc. 150 (2003) A1457–A1464.
[3] V.P. Phan, PhD thesis, University of Bordeaux (2009).
[4] W.-J. Zhang, J. Power Sources 196 (2011) 13–24.
[5] Y.M. Lee, J.Y. Lee, H.-T. Shim, J.K. Lee, J.-K. Park, J. Electrochem. Soc. 154 (2007) A515–A519.
[6] C.K. Chan, R. Ruffo, S.S. Hong, Y. Cui, J. Power Sources 189 (2009) 1132–1140.
[7] D. Aurbach, J. Power Sources 89 (2000) 206–218.
[8] K. Xu, Chem. Rev. 104 (2004) 4303–4418.
[9] H. Ota, Y. Sakata, A. Inoue, S. Yamaguchi, J. Electrochem. Soc. 151 (2004) A1659–A1669.
[10] S.S. Zhang, J. Power Sources 162 (2006) 1379–1394.
[11] H. Lee, S. Choi, S. Choi, H.-J. Kim, Y. Choi, S. Yoon, J.-J. Cho, Electrochem. Commun. 9 (2007) 801–806.
[12] L. Chen, K. Wang, X. Xie, J. Xie, J. Power Sources 174 (2007) 538–543.
[13] N.-S. Choi, K.H. Yew, K.Y. Lee, M. Sung, H. Kim, S.-S. Kim, J. Power Sources 161 (2006) 1254–1259.
[14] G.-B. Han, M.-H. Ryou, K.Y. Cho, Y.M. Lee, J.-K. Park, J. Power Sources 195 (2010) 3709–3714.
[15] G.-B. Han, J.-N. Lee, J.-W. Choi, J.-K. Park, Electrochim. Acta 56 (2011) 8997–9003.
[16] L. Martin, H. Martinez, M. Ulldemolins, B. Pecquenard, F. Le Cras, Solid State Ionics, under review.
[17] L. El Ouatani, R. Dedryvère, C. Siret, P. Biensan, S. Reyanud, P. Iratçabal, D. Gonbeau, J. Electrochem. Soc. 156 (2009) A103–A113.
[18] J. Li, A.K. Dozier, Y. Li, F. Yang, Y.-T. Cheng, J. Electrochem. Soc. 158 (2011) A689–A694.
[19] Y. Oumellal, N. Delpuech, D. Mazouzi, N. Dupré, J. Gaubicher, P. Moreau, P. Soudan, B. Lestriez, D. Guyomard, J. Mater. Chem. 21 (2011) 6201–6208.